Oxygen-molecule spin-nanotubes constructed by physisorption into a nanoporous medium

Masaki Mito,[1,2,*] Noritoshi Shinto,[1] Yuki Komorida,[1] Takayuki Tajiri,[3] Hiroyuki Deguchi,[1,2] Seishi Takagi,[1] and Shigemi Kohiki[1]

[1]*Faculty of Engineering, Kyushu Institute of Technology, Kitakyushu 804-8550, Japan*

[2]*CREST, Japan Science and Technology Agency (JST), Saitama 332-0012, Japan*

[3]*Faculty of Science, Fukuoka University, Fukuoka 814-0180, Japan*

(Received 27 March 2008; published 29 August 2008)

We succeeded in controlling gas-liquid-solid transitions and in constructing "spin-nanotubes (SNTs)" based on antiferromagnetic correlations by physisorbing oxygen molecules (O_2) into the nanosize pores of a mesoporous medium MCM-41 while also manipulating the adsorption quantity. The phase diagram of O_2 physisorbed into MCM-41 presents many common characteristics with that of O_2 layers physisorbed on graphite substrates. In the present case, experimental verification of the antiferromagnetic square lattice in the liquid phase of the monolayer proved the formation of O_2 SNTs. The present O_2 SNT is an experimental example of the successful construction of SNT.

DOI: 10.1103/PhysRevB.78.064428 PACS number(s): 75.75.+a, 75.50.Xx, 75.40.Cx

I. INTRODUCTION

In nature, oxygen forms molecules consisting of two atoms of the same element. The molecule orbital is characterized by a parallel arrangement of two spins on two degenerated antibonding $2p_\pi$ orbitals, resulting in a magnetic nature with the spin $S=1$. The magnetic susceptibility of the oxygen molecule (O_2) was first measured by Kamerlingh Onnes and Perrier[1] in 1914. Nowadays, all the magnetic properties of the oxygen molecule are widely known thanks to past studies:[2–5] the gas phase exhibits paramagnetism whereas antiferromagnetic (AFM) intermolecular interaction develops in the liquid phase (below 90.2 K). Interestingly, the color of the liquid phase is blue. In the solid phase (below 55.4 K), there are three structurally nonequivalent phases: α, β, and γ. The cubic γ phase (43.8–55.4 K) exhibits a one-dimensional (1D) AFM correlation with $J_\gamma/k_B=14$ K, defined by the Hamiltonian $2JS_i \cdot S_j$. The rhombohedral β phase (23.9–43.8 K) with a hexagonal plane structure is a two-dimensional (2D) AFM system with $J_\beta/k_B=22$ K. The monoclinic α phase ($\leqq$24 K) with magnetic ordering is a quasi-2D system with $J_\alpha/k_B=30$ K on the *ab* plane and the easy axis is the *b* axis. In the present study, we investigated the effects of confining the mobility of O_2 and manipulating the molecule number on the above-mentioned properties through adsorption experiments into a mesoporous medium. We expect that confinement will induce different properties in known materials through the manipulation of dimensionality.

In the past, there have been many experiments on O_2 adsorption into mesoporous media such as zeolites (pore diameter: $D<0.8$ nm), organic Cu-metal coordination (CMC) materials ($D=0.5-0.7$ nm),[6–8] and graphite[9–11] or boron nitride substrates.[11] However, these studies had some problems: both zeolites and organic CMC materials contain cations, resulting in a gas adsorption potential with a local energy minimum. As for CMC, the medium itself becomes magnetically active, and magnetic as well as electric interactions between O_2 and the medium are inevitable. Furthermore, the adsorption capacity of O_2 is restricted to a few molecules per cross section in both systems. As for the adsorption on graphite or boron nitride substrates, magnetic properties have been studied in detail over the wide region as monolayer→bilayer→bulk state. The studies, however, have been limited to the condensation phase. Thus, it has been impossible so far to widely manipulate the molecule number across the entire phase range from gas to solid.

The mesoporous silica, MCM-41,[12] which we chose as the best medium, has pores of $D=3.0$ nm and contains no cations, resulting in a clean adsorption potential and a large adsorption capacity. The pores are arranged regularly, forming a hexagonal closed packing structure. The van der Waals diameter of O_2 is estimated to be about 0.4 nm based on the Lennard-Jones potential. According to Ref. 5, the ellipsoidal long axis is calculated to be 0.42 nm. One can suppose that the pores allow the physisorption of not more than 42 molecules per section, as shown in Fig. 1(a). The layer structure may consist of three layers and some additional material. According to the results of a study on ^{4}He molecules confined in MCM-41, the first layer is solid, the second is solid or liquid, and the third is liquid at low temperatures.[13] In the present case, since the van der Waals force between the O_2 molecules is much larger than that between ^{4}He molecules, the solid phase may be stably established in the second and third layers. Furthermore, by manipulating the adsorption quantity into MCM-41, one can change the dimensionality of the spin system as follows: zero-dimensional (0D)→dirty 1D→2D, as Fig. 1(b) → multilayer tube, quasi 2D close to three-dimensional (3D). The present phase diagram of O_2 obtained in the condensed state presents many common characteristics with that of 2D layered system physisorbed on graphite substrates.[10,11] Although the condensation in pores with diameter of 3.0 nm gives quasi-1D confinement to O_2 molecules, fine 2D magnetic feature was observed in an adequate filling range. There the monolayer tube structure is probably realized, and we consider the unique status as the formation of "O_2 SNTs" with both quasi-1D structural confinement and 2D magnetic nature.

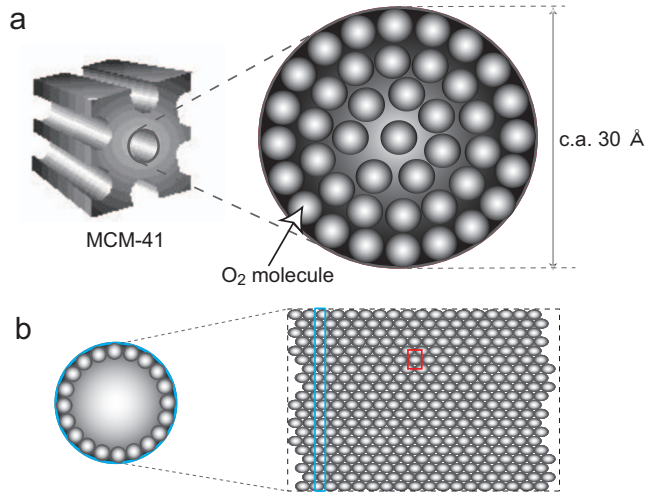

FIG. 1. (Color) Hypothetical schematic of an oxygen molecule (O_2) adsorbed into a pore of MCM-41. The diameter of the pore is about 3.0 nm. The walls between the pores have a thickness of about 1.0 nm. (a) Vertical section of MCM-41 into which 42 oxygen molecules with a van der Waals diameter of 0.4 nm are adsorbed per section. There is a multilayer structure consisting of three layers and some additional material. The number of adsorbed molecules in the first, second, and third layers are 20, 14, and 8 per section, respectively. (b) Conceptual view of the tube opened along its length. Ellipsoidal O_2 molecules seem to be aligned along the wall rather than perpendicularly to it. The blue circle on the left corresponds to the sectional view of the blue area in the rectangle on the right. The red square is a unit cell of the square lattice with four nearest-neighboring molecules.

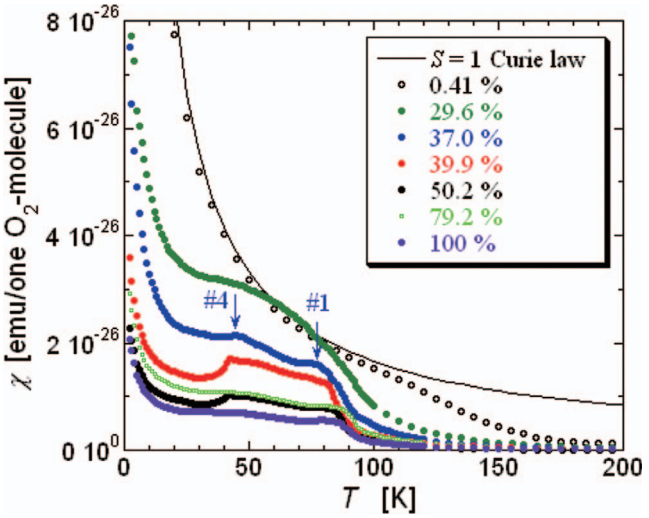

FIG. 2. (Color) Temperature dependence of the magnetic susceptibility, $\chi(T)$, of O_2 adsorbed into MCM-41. χ stands for the dc magnetic susceptibility normalized per one molecule. The solid curve represents the Curie law for $S=1$. The anomalies of #1 and #4 are related with vaporization and melting of the first layer, respectively.

II. EXPERIMENT

The adsorption experiment was filled at room temperature according to the following procedure. First, the adsorption quantity, N, of O_2 was calculated from the vacuum volume of the Pyrex glass tube used and the pressure of the O_2 gas (1.1–1.3 atm). Next, the pore volume, V, of MCM-41 with $D=3.0$ nm was calculated from the mass (3.5–40.8 mg) and the pore volume per unit mass [0.73 cm^3/g (Refs. 14 and 15)]. Here, the value of D was estimated by x-ray diffraction measurement. Finally, the filling ratio, n, of O_2 in MCM-41 was estimated from N/V. The experimental error of the estimated value of n is below 5% of the estimated one. Since individual pores are parted with the nonmagnetic wall of width of 1.0 nm, the interaction between O_2 molecules in different pores is negligible.

The temperature (T) dependence of the magnetization (M) at a magnetic field (H) of 1 T was studied using a commercial superconducting quantum interference device (SQUID) magnetometer. In the perfect filling ($n=100\%$), the magnetization measurements were performed at both $H=1$ and 3 T. So as to prevent local condensation, the sample was cooled from 130 to 2 K over a period of 275 min. At $T<100$ K, the adsorption quantity of O_2 into MCM-41 became saturated. In all of the measurements, $M(T)$ was observed in both the cooling and the heating processes, and it was confirmed that there was no distinct difference between the two $M(T)$ values in the condensed states. In some filling ratios, reproducibility was confirmed by running the same experiment twice. We define the M/H per molecule as the normalized susceptibility, χ, in order to find out the intrinsic characteristic of the entire filling region and present the results for the heating process.

As described later, the phase diagram of the condensation state of O_2 physisorbed into MCM-41 is quite similar to that on graphite substrates.[10,11] Thus, as for the naming of each state, we referred to the naming in Murakami and co-worker's[10,11] study using the graphite substrates.

III. EXPERIMENTAL RESULTS AND DISCUSSION

Figure 2 shows the $\chi(T)$ curve over the entire filling region. The enlarged figures in the range of 0–70 K and 60–110 K are shown in Figs. 3(a) and 4, respectively. As seen in Fig. 2, at the low n of 0.41%, $\chi(T)$ accords with the Curie law for $S=1$. This suggests that each molecule behaves paramagnetically in dilute gas. Here, we stress the quantitative consistency of $\chi(T)$ between the experimental data and the value predicted by the Curie law; this agreement guarantees that the above-mentioned evaluation method for n is adequate. As n increases, the $\chi-T$ curve deviates from the Curie law and the magnitude of χ is gradually suppressed. For $n>20\%$, which corresponds to the filling of almost half of the first layer, a broad hump due to AFM short-range ordering appears at around 50 K. Actually, up to $n=30\%$, there appear no distinct transitions in any condensed phase in the filling region. At $n>25\%$, molecular contact becomes inevitable even when assuming that O_2 molecules diffuse uniformly in MCM-41. Indeed, at $n=37.0\%$, vaporization (#1 in Fig. 2) and meltinglike transitions (#4) were observed at around 80 and 45 K, respectively. The $\chi(T)$ curve at $n=39.9\%$ [see Fig. 3(a)] indicates a conspicuous transition

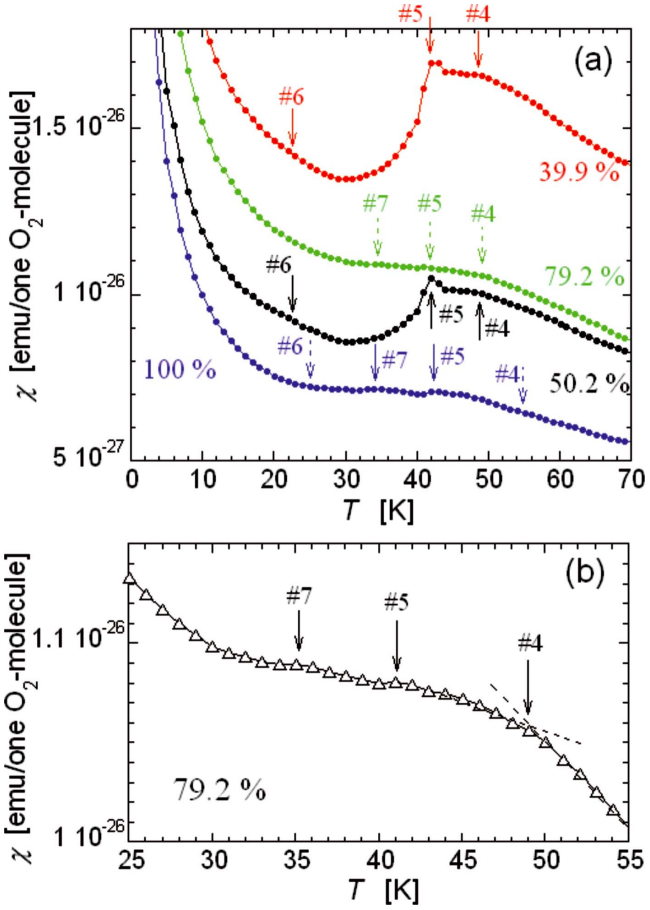

FIG. 3. (Color online) (a) Temperature dependence of $\chi(T)$ of O_2 adsorbed into MCM-41 in the condensation state. The anomalies are labeled as #4–#7. The solid arrows indicate the distinct anomalies confirmed in the present figures while the broken arrows indicate small anomalies that can be detected by further enlarging these figures. In (b), the data of $n=79.2\%$ are enlarged in the temperature region of 25–55 K.

(#5) near 42 K and, at a slightly higher temperature, a kink of #4 was detected. The anomaly of #4 probably represents the fluid I-fluid II transition seen in the physisorption on graphite substrates.[11] According to Ref. 11, fluid I is a normal liquid phase while fluid II does not have a random distribution of the molecule axis. However it maybe losing the translation symmetry, and is considered to be a quasistable state between liquid and solid ones. At higher filling states, fluid II is assumed to lead to the γ phases of the solid. Furthermore, at $n=39.9\%$, the magnetic transition (#6) is detected at around 22 K and it corresponds to the $\varepsilon-\zeta$ transition seen in the physisorption on graphite substrates. The characteristic signal more distinctly appears near 20 K at $n=50.2\%$ [see Fig. 3(a)], which almost corresponds to the perfect filling of the first layer.

The adsorption state at $n>50\%$ should be regarded as a quasi-2D system with unstable condensation resulting in random exchange fields between the first and second layers. Careful observation reveals the existence of successive vaporization in a blurred anomaly around 80–90 K (see Fig. 4). Here, #1–#3 probably correspond to the vaporization in the

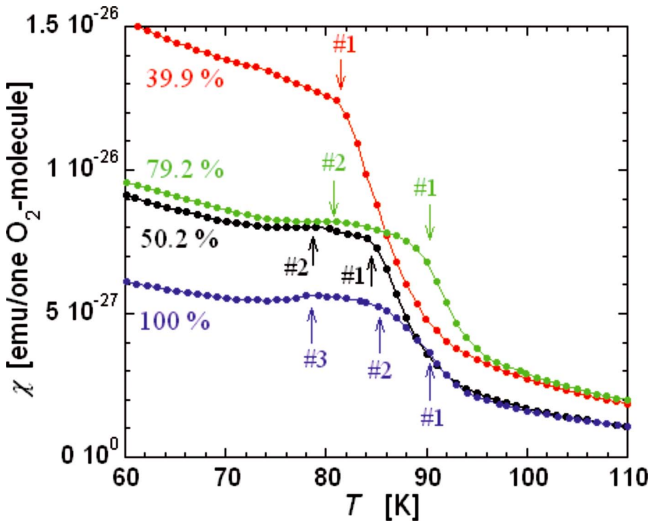

FIG. 4. (Color online) Temperature dependence of $\chi(T)$ of O_2 adsorbed into MCM-41 near the vaporization. The anomalies of #1–#3 might represent the vaporization of the first, second, and third layers, respectively.

first, second, and third layers, respectively, whereas, in the condensed state below 60 K, it is difficult to distinguish these transitions. According to a previous study on the adsorption of O_2 on graphite, the adsorption on the second layer rendered the magnetic ordering of the first layer unstable whereas magnetic ordering was stabilized again as the bulk-system state was approached with further adsorption.[10,11] The above scenario convinces us that there is no anomaly in #6 at $n=79.2\%$, as shown in Fig. 3(a). Furthermore, at $n>50\%$, a small hump appears in #7 around 35 K, which seems to originate in the melting transition of the second and/or third layers [see Figs. 3(a), 3(b), and 5(c)].

Figure 5 shows the $\chi(T)$ curve at the perfect filling, $n=100\%$, for $H=1$ and 3T. There the influence by increasing magnetic field is hardly seen. The four transition temperatures, labeled as #1 and #4–#6, detected there coincide with those of the liquid-gas, solid (γ)-liquid, $\beta-\gamma$, and $\alpha-\beta$ transitions in the bulk system, respectively. As mentioned above, #2, #3, and #7 seem to correspond to the condensation of the second and third layers. In the ^{4}He physisorption into MCM-41, the solid state in the second layer was not completed.[13] The existence of #7 might originate because the van der Waals force between O_2 molecules is larger than that between ^{4}He molecules. Thus, one can see the crossover from the dilute gas system to the bulk system. We have been able to observe the change of molecular condensation by controlling the adsorption quantity from the gas region systematically.

Figure 6(a) shows the phase diagram of O_2 molecule physisorbed into MCM-41. For reference, the phase diagram of the 2D sheet system via the O_2 physisorption on graphite substrates[11] is shown in Fig. 6(b). The characteristics of the 2D sheet system are as follows: (1) the existence of ε, ζ, and fluid II phases, leading to the α, β, and γ phases in the bulk system, and (2) the disappearance of the magnetic order (ε phase) in the dense bilayer state. Interestingly all of these characteristics were also seen in the present physisorption

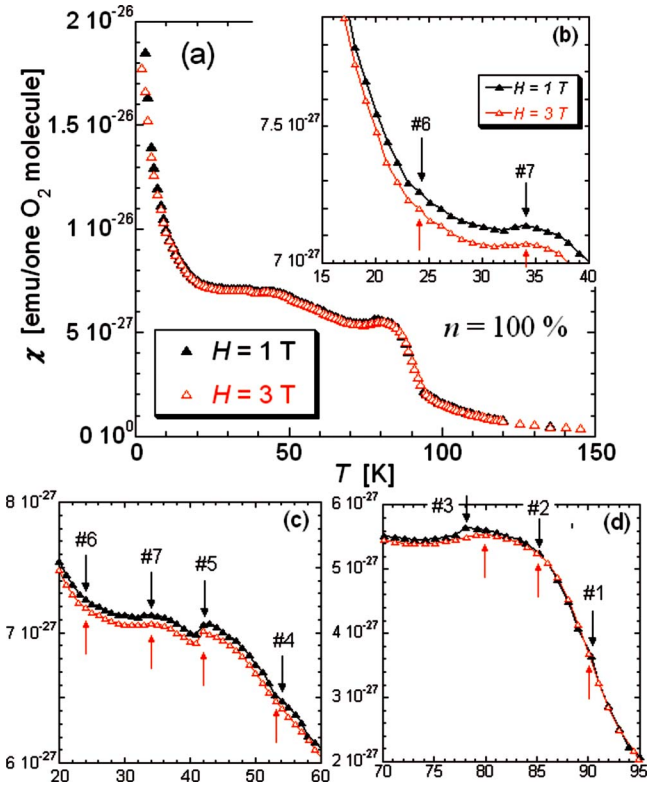

FIG. 5. (Color online) (a) Temperature dependence of $\chi(T)$ of O_2 adsorbed into MCM-41 at the perfect filling state, $n=100\%$ for $H=1$ and 3 T. The data in the solid state, near the melting, and near the vaporization are enlarged in (b), (c), and (d), respectively.

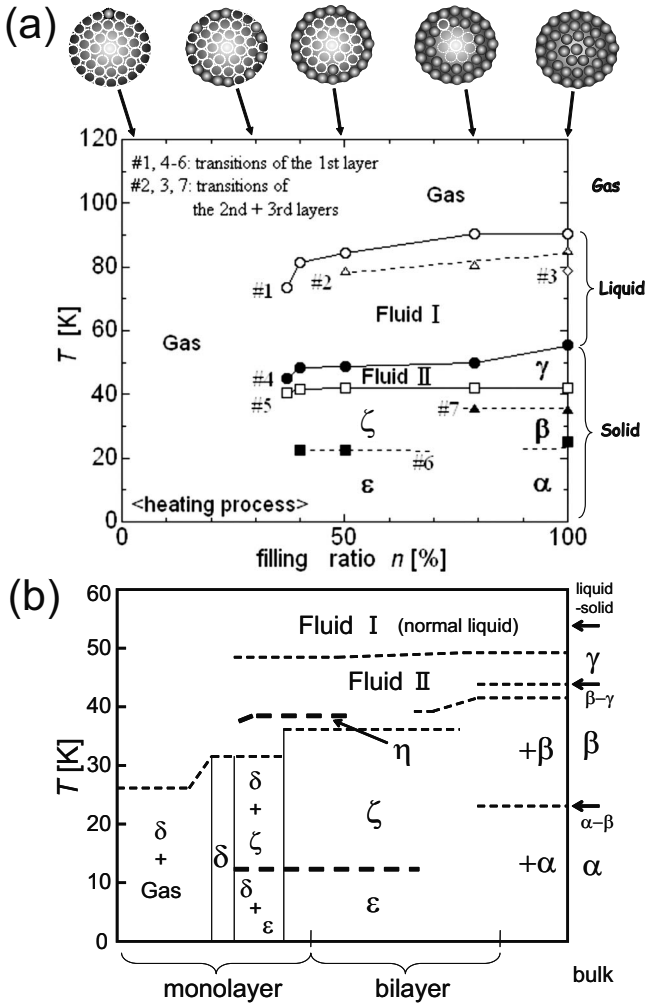

FIG. 6. (a) Phase diagram of O_2 adsorbed into MCM-41. An imaginary adsorption state is depicted along with representative filling ratios. With increasing the filling ratio, the curves #1 and #4–#6 lead to the liquid-gas, solid (γ)-liquid, $\beta-\gamma$, and $\alpha-\beta$ transitions in the bulk system, respectively. The curves #2 and #7 seem to correspond to the vaporization and melting transitions of the second layer, respectively. The #3 curve may represent the vaporization in the third layer. As for the naming of each phase, we referred to the naming in Murakami and co-worker's (Refs. 10 and 11) study using the graphite substrates. (b) Phase diagram of O_2 adsorbed on the graphite substrates (Ref. 11). Figure 7 of Ref. 11 was modified so as to be easily compared with the result of Fig. 6(a) of the present paper. The horizontal axis represents relative coverage in the monolayer, bilayer, and bulk.

experiment in the present tube system. Herein, as for the naming of each phase in Fig. 6(a), we referred to the naming of the corresponding phase in Fig. 6(b).

Next, we discuss the dimensionality of the spin system and the strength of the net exchange interaction, J, based on our analyses using a theoretical solution.[16] Figure 7 shows the analysis results for $n=37.0\%$, 39.9%, and 50.2%. The state in which more than 70% of the first layer is occupied can be theoretically regarded as a 2D system with a density exceeding the percolation density. Here, the number of the nearest-neighboring molecules is z. In the liquid phase, the orientation of the O_2 molecules adsorbed on the inner walls of MCM-41 should be random but ellipsoidal molecules seem to be aligned along the wall, as suggested in the low-coverage adsorption on graphite.[11] Thus, it is unreasonable to consider a triangular lattice ($z=6$) with the highest occupation density in a 2D system due to anisotropic condensation. Consequently, the analysis based on the square lattice ($z=4$) model gave the best fit, as shown in Fig. 7. The data for $\chi(T)$ in the liquid phase for $n=37.0\%$ and 39.9% could be reproduced by the theoretical calculation of the square lattice[16] with $J/k_B=5.1$ and 7.5 K, values which are reasonably smaller than the J_γ of the bulk system. Murakami and co-workers[10,11] have reported that, in the O_2 physisorption on the graphite substrates, the neutron-diffraction measurements presented the next-nearest-neighbor interaction (J_{NNN}) with about a half of nearest-neighbor interaction (J_{NN}) in the monolayer. Indeed, J_{NNN} and small anisotropy (D) effects due to the dipolar and molecular origins may have to be considered in the spin Hamiltonian; but herein it is quite difficult to discuss the effects of J_{NNN} and D in addition to J_{NN} in the analysis of the present $\chi(T)$ data. Anyway, the existence of the 2D spin system has been successfully verified via nice reproduction with the theoretical calculation of square lattice. We conclude that the artificial construction of O_2 SNTs was successful.

Similar 2D nature has been confirmed in the solid phase in the bulk and 2D layer systems.[5,10,11] The present observation of 2D magnetic nature in the liquid phase originates from the use of adsorption medium with the tube structure.

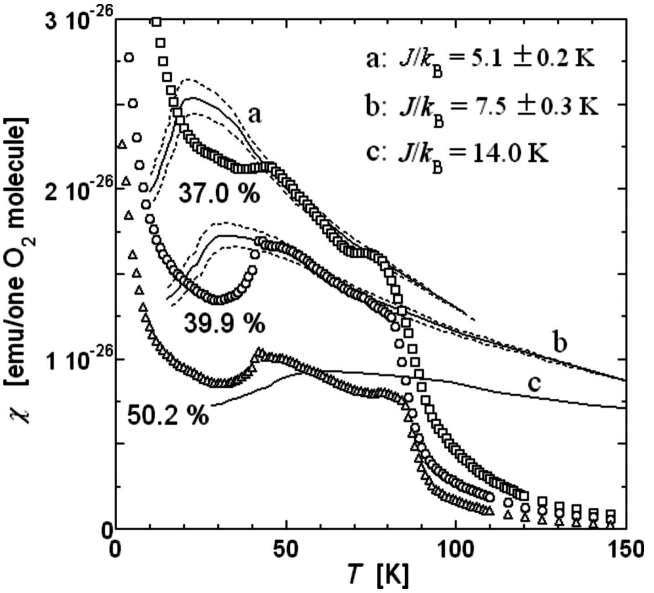

FIG. 7. [(a)–(c)] Quantitative analysis of $\chi(T)$ for the adsorbed state at the filling ratio of 37.0%, 39.9%, and 50.2%, using a two-dimensional square lattice model with $S=1$. The AFM exchange interaction, J/k_B, is defined by the Hamiltonian $2JS_i \cdot S_j$.

Furthermore, let us mention the paramagnetic increase in χ below 20 K seen in all data of Fig. 2. When the paramagnetic component was quantitatively analyzed based on the paramagnetic spin of $S=1$, the percentage was about 10%, 5%, and 1% for $n=29.6\%$, 37.0%, and 100%, respectively. In $n=100\%$, the paramagnetic component should be due to the O_2 molecule adsorbed on the surface of MCM-41. The monolayer growth in physisorption might proceed by island growth due to the net attractive long-range interaction between adsorbate molecules. The slow cooling from room temperature must disturb the development of localized large island. Consequently in an incomplete filling state of monolayer, there are some vacancy sites, resulting in the effective site dilution. The resultant percolation effects should bring about the paramagnetic behavior, which might be a characteristic of dilute SNT. We think that 2D nature should survive even in the solid phase for $n=37.0\%$ and 39.9%, whereas the jump of magnetic response due to the melting and the large paramagnetic contribution make it difficult to confirm the 2D nature by reproduction with the theoretical model.

At $n>50\%$, it is difficult to reproduce the $\chi(T)$ data using a specific theoretical model. Interestingly, there is no pronounced deviation between the magnetic signals at $n=50.2\%$ and 79.2%, as shown in Fig. 2. A simple calculation shows that there is no distinct difference between the averaged values of z for the two states. This phenomenon also corroborates the many-body effect.

Similar experiment has been already performed by our group using the mesoporous silica SBA-15 with $D=7.8$ nm. In the filling of 10.2% (about 50% of the monolayer), the broad hump due to the short-range magnetic order appeared with more prominent curvature than those of $n=26.4\%$ (about 56% of monolayer) and $n=29.6\%$ (about 60% of monolayer) in the present experiment using MCM-41 because of the enlargement of correlation length. However, we could not succeed in the nice reproduction of $\chi-T$ data with the 2D theoretical calculation, suggesting that it is difficult to form the uniform adsorption state in SBA-15. In this sense, the pore size of 3.0 nm in MCM-41 might be suitable for realizing the adsorption state with the equal diffusion percentage.

As for similar experiment using a $S=1/2$ magnetic gas, we have performed the experiment of physisorbing NO gas into MCM-41. The NO molecule has the electric polarity, resulting in the formation of nonmagnetic N_2O_2 molecule in the solid state below 110 K even at a state of extremely low filling. We could not observe the magnetic characteristic of the $S=1/2$ spin system at lower temperatures.

On the theoretical side, the study of SNTs based on the ladder structure has already started.[17] The successful results on the dimensionality and exchange interaction in the tube system should serve as a strong incentive to theoretical scientists.

IV. CONCLUSION

In summary, our experiment of O_2 physisorption into MCM-41 allowed us to discover properties of O_2 in terms of both the van der Waals force and the magnetic interactions. The most impressive result is the verification of the construction of O_2 SNTs in the liquid state of the dense monolayer region based on the analysis of $\chi(T)$. Furthermore the condensation process of O_2 was investigated in the wide phase range from gas to solid by manipulating the molecule number. The condensed states such as liquid and solid appeared in the state with three-fourths filling of the first layer, and present the phase change similar to that of O_2 physisorbed on the graphite substrates against the increase in the molecule number. The resultant percolation effects for the medium filling in the first layer brought about the meaningful paramagnetic behavior, which might be a characteristic of dilute SNT. Carbon nanotubes are nonmagnetic. We expect the present findings related to our experimental SNT system to accelerate the development of the research field of SNTs, especially on the theoretical side.

ACKNOWLEDGMENTS

This work was supported by the CREST project of the Japan Science and Technology Corporation (JST).

*mitoh@tobata.isc.kyutech.ac.jp

[1] H. Kamerlingh Onnes and A. Perrier, Comm. Phys. Lab. Leiden **139c**, 25 (1914).
[2] E. Kanda, T. Haseda, and A. Otsubo, Physica (Amsterdam) **20**, 131 (1954).
[3] G. C. DeFotis, Phys. Rev. B **23**, 4714 (1981).
[4] R. J. Meier, C. J. Schinkel, and A. de Visser, J. Phys. C **15**, 1015 (1982).
[5] C. Uyeda, K. Sugiyama, and M. Date, J. Phys. Soc. Jpn. **54**, 1107 (1985).
[6] W. Mori, T. C. Kobayashi, J. Kurobe, K. Amaya, Y. Narumi, T. Kumada, K. Kindo, H. A. Katori, T. Goro, N. Miura, S. Takamizawa, H. Nakayama, and K. Yamaguchi, Mol. Cryst. Liq. Cryst. **306**, 1 (1997).
[7] R. Kitaura, S. Kitagawa, Y. Kubota, T. C. Kobayashi, K. Kindo, Y. Mita, A. Matsuo, M. Kobayashi, H.-C. Chang, T. C. Ozawa, M. Suzuki, M. Sakata, and M. Takata, Science **298**, 2358 (2002).
[8] T. C. Kobayashi, A. Matsuo, M. Suzuki, K. Kindo, R. Kitaura, R. Matsuda, and S. Kitagawa, Prog. Theor. Phys. Suppl. **159**, 271 (2005).
[9] U. Kobler and R. Marx, Phys. Rev. B **35**, 9809 (1987).
[10] Y. Murakami and H. Suematsu, Phys. Rev. B **54**, 4146 (1996).
[11] Y. Murakami, J. Phys. Chem. Solids **59**, 467 (1998).
[12] C. T. Kresge, M. E. Leonowicz, W. J. Roth, J. C. Vartuli, and J. S. Beck, Nature (London) **359**, 710 (1992).
[13] F. Albergamo, J. Bossy, H. R. Glyde, and A.-J. Dianoux, Phys. Rev. B **67**, 224506 (2003).
[14] M. Selvaraj, P. K. Sinha, K. Lee, I. Ahn, A. Pandurangan, and T. G. Lee, Microporous Mesoporous Mater. **78**, 139 (2005).
[15] M. Kruk, M. Jaroniec, Y. Sakamoto, O. Terasaki, R. Ryoo, and C. H. Ko, J. Phys. Chem. B **104**, 292 (2000).
[16] Y. J. Kim and R. J. Birgeneau, Phys. Rev. B **62**, 6378 (2000).
[17] For example, A. Lüscher, R. M. Noack, G. Misguich, V. N. Kotov, and F. Mila, Phys. Rev. B **70**, 060405(R) (2004).